Enhanced ferroelectric and piezoelectric properties in doped lead-free $(Bi_{0.5}Na_{0.5})_{0.94}Ba_{0.06}TiO_3$ thin films

D. Y. Wang,[1,a)] N. Y. Chan,[2] S. Li,[1] S. H. Choy,[2] H. Y. Tian,[3] and H. L. W Chan[2]
[1]*School of Materials Science and Engineering, The University of New South Wales, Sydney, New South Wales 2052, Australia*
[2]*Department of Applied Physics and Materials Research Centre, The Hong Kong Polytechnic University, Hung Hom, Kowloon, Hong Kong*
[3]*Department of Imaging and Applied Physics, Curtin University of Technology, GPO Box U 1987, Perth, WA 6845, Australia*

(Received 24 June 2010; accepted 23 October 2010; published online 22 November 2010)

Doping effects with respect to the electrical properties of morphotropic phase boundary $(Bi_{0.5}Na_{0.5})_{0.94}Ba_{0.06}TiO_3$ thin films epitaxially grown on $CaRuO_3$ electroded $(LaAlO_3)_{0.3}(Sr_2AlTaO_6)_{0.35}$ (001) substrates were investigated. Substantial enhancement of ferroelectricity and piezoelectricity has been achieved in La+Ce codoped films with a remanent polarization P_r of 29.5 $\mu C/cm^2$ and a remanent piezoelectric coefficient $d_{33,f}$ of 31 pm/V, whereas Mn doping seems more favorite to reduce the leakage current by two order of magnitude. Both doped films exhibited diodelike *I-V* characteristics, which are correlated with resistance switching effect. © *2010 American Institute of Physics*. [doi:10.1063/1.3518484]

Due to the increasing environmental and biological concerns on high toxicity of lead present in the widely used $Pb(Zr,Ti)O_3$ (PZT) family, considerable attention has been drawn to develop lead-free ferroelectric materials in the past two decades.[1] Among various potential lead-free piezoelectric ceramics, *A*-site complex perovskite $(Bi_{0.5}Na_{0.5})TiO_3$ (BNT) is considered to be one of the strong candidates because of its marked ferroelectricity/piezoelectricity.[2,3] The pioneer work by Takenaka *et al.*[4] demonstrated that rhombohedral (F_α)-tetragonal (F_β) morphotropic phase boundary (MPB) in $(Bi_{0.5}Na_{0.5})TiO_3-BaTiO_3$ (BNBT) binary system is remarkably effective in promoting piezoelectric properties. Subsequent studies revealed the piezoelectric performance of BNBT ceramics with MPB composition could be further enhanced by appropriate dopants.[5–7]

In spite of the numerous studies on BNT-based single crystals and ceramics, literature tackling with the growth and characterization of BNT-based, especially BNBT-based thin films, still remains at an infancy stage.[8–12] Consequently, doping effects on the electrical properties of thin film BNBT materials are still unclear. Abazari *et al.*[13] has recently reported epitaxial potassium modified BNBT thin films grown on $SrRuO_3$ coated $SrTiO_3$ substrates by pulsed laser deposition (PLD). Dielectric and piezoelectric properties of the films were evaluated macroscopically. However, the nanoscale characterization of piezoresponse of doped BNBT thin films is still missing. In this letter, thin films of La+Ce codoped and Mn-doped BNBT with composition in the vicinity of MPB are epitaxially deposited on $CaRuO_3$ (CRO) electroded $(LaAlO_3)_{0.3}(Sr_2AlTaO_6)_{0.35}$ (LSAT) (001) single-crystal substrates by PLD. Effects of dopants on ferroelectric, dielectric, leakage current, and local piezoelectric properties of the BNBT-based thin films are investigated.

The 10% Bi-enriched targets of $(Bi_{0.5}Na_{0.5})_{0.94}Ba_{0.06}TiO_3$+0.5 mol % CeO_2+0.5 mol % La_2O_3 (BNBT-LaCe), $(Bi_{0.5}Na_{0.5})_{0.94}Ba_{0.06}TiO_3$+0.5 mol % MnO_2 (BNBTMn) used for laser ablation were fabricated by the conventional solid state reaction route. The substrates were cubic (001)-oriented LSAT (a=3.868 Å), which were first coated a layer of CRO (~40 nm) by PLD. CRO was chosen as bottom electrode material not only because of its high electrical conductivity in comparison with widely used $SrRuO_3$,[14] but also because its high lattice similarity[15] with LSAT and BNBT (rhombohedral, a=3.893 Å). The BNBT-LaCe and BNBTMn thin films were grown on $CRO(001)_c/LSAT(001)$ by PLD using a KrF excimer laser (Lambda Physik COMPex 205, Göttingen, Germany) with a repetition rate of 10 Hz. The laser beam impacts the rotating target with an energy density of 2 J/cm^2. The distance between the target and the substrate was fixed at 5 cm, while the oxygen ambient pressure was maintained at 35 Pa during laser ablation. The substrate temperature for deposition was kept at 640–650 °C for all the films. An undoped BNBT thin film was also deposited on $CRO(001)_c/LSAT(001)$ under the same conditions for comparison purpose. The films were grown to a thickness of ~380 nm to minimize the strain effects. After deposition, the as-grown thin films were *in situ* annealed at 650 °C under 1 atm pure oxygen for 5 min, and then gradually cooled down to room temperature. Circular Au top electrodes with diameter of 250 μm were prepared by rf magnetron sputtering through a shadow mask, prior to the measurement of electrical properties.

Figure 1 shows the X-ray diffraction (XRD, Bruker AXS D8 Discover, Madison, WI) θ-2θ spectra of BNBT-based thin films. Only strong (00l) peaks appear in the spectra, indicating the appearance of pure perovskite phase. The in-plane alignment of the thin films with respect to the major axes of the (001) substrates was also confirmed by the XRD off-axis φ scan of the (202) reflections, as shown in the insets of Fig. 1. Appearance of four peaks with 90° interval indicates a cube-on-cube epitaxial growth relationship between the films and substrates. Lattice parameters (out-of-

a)Author to whom correspondence should be addressed. Tel.: +61 02 9385 4440. FAX: +61 02 9385 5956. Electronic mail: dy.wang@unsw.edu.au.

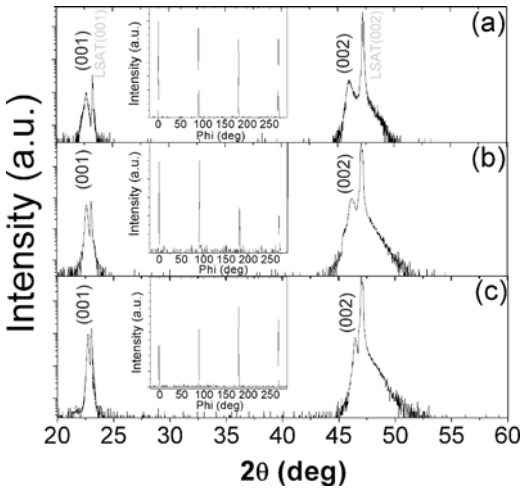

FIG. 1. (Color online) XRD θ-2θ scans of (a) BNBTLaCe, (b) BNBTMn, and (c) BNBT thin film epitaxially grown on CRO$(001)_c$/LSAT(001) substrates. Insets are the off-axis φ scans of the (202) reflections of corresponding films.

plane c, in-plane a) and c/a ratios of the thin films were determined from the XRD results. The c/a ratios were found to be 1.0066 ± 0.0002, 1.0019 ± 0.0003, and 1.0001 ± 0.0002 for BNBTLaCe, BNBTMn, and BNBT thin films, respectively. This indicates the lattice of doped BNBT thin films are tetragonally distorted, while the undoped BNBT thin film remains a rhombohedral structure, which is in good agreement with previously reported results by other groups.[9]

Ferroelectric hysteresis (P-E) loop was measured using a TF Analyzer 2000 equipped with a FE-Module (aixACCT, Aachen, Germany). Well-defined P-E hysteresis loops are observed for all films, at 1 KHz, as shown in Fig. 2. The remnant polarization P_r and coercive field E_c are 29.5 μC/cm^2 and 7.4 kV/mm, 24.5 μC/cm^2 and 11.3 kV/mm, and 14.5 μC/cm^2 and 10.2 kV/mm for BNBTLaCe, BNBTMn, and BNBT thin films, respectively. It should be noted that P_r of doped films are comparable to bulk values, whereas the E_c values are considerable higher, which may be attributed to the size effect.[16] In general, tetragonality (c/a) is strongly correlated with ferroelectric properties in perovskite oxides. It is believed that the increased c/a ratio in doped thin films contributes to their enhanced ferroelectricity. The inset of Fig. 2 illustrates the C-V characteristics of the BNBT-based films measured using an Agilent 4292A impedance analyzer (Agilent Tech., Santa Clara, CA) at 1 MHz. The hysteretic nonlinearity of ε on the dc bias field demonstrates that the ferroelectric properties of the films were originated from the domain switching. In addition, the dielectric permittivity ε at zero electric field has been significantly enhanced by the dopants, from 340 for undoped film to 395 and 480 for BNBTMn and BNBTLaCe thin films, respectively. Ce^{3+} and La^{3+} go into A-site to create A-site vacancies, which facilitate the movement of domain wall, so as to increase the ferroelectric and dielectric properties. Nevertheless, multivalent Mn (Mn^{2+}, Mn^{3+}, and Mn^{4+}) may coexist in perovskite oxide thin films[17] and possibly occupy either A- or B-sites.[18] The simultaneous enhancement of polarization, dielectric permittivity, and coercive field caused by Mn doping implies that Mn may act as both "softening" and "hardening" dopant.

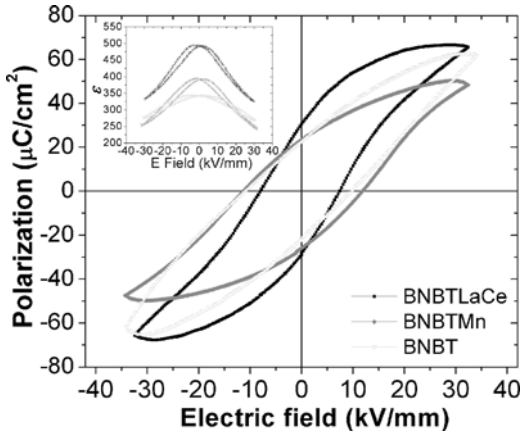

FIG. 2. (Color online) P-E hysteresis loops of the epitaxial BNBT-based thin films. Their electric field dependence of dielectric permittivity is shown in the inset.

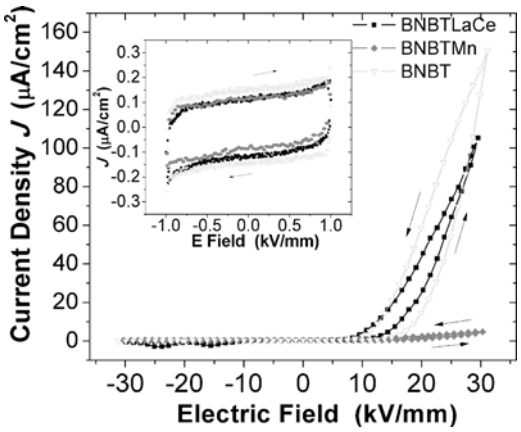

FIG. 3. (Color online) Leakage current density J as a function of electric field E for the Au/BNBT-based thin film/CRO capacitors at room temperature. Inset is the J-E characteristics at low electric field.

The leakage currents through the BNBT-based thin film capacitors were measured using a Keithley 6517A programmable electrometer (Keithley, Cleveland, OH). Figure 3 gives the typical I-V curves of the Au/ film/CRO heterostructures. All the films show diodelike I-V characteristics with hysteresis and the leakage current is limited at the film/CRO interface. The loss of A-site volatile elements, e.g., Na^+ and Bi^{3+}, implies that BNBT-based thin films exhibit p-type conductivity, while CRO is n-type. Similar I-V characteristics subject to resistance switching has been also observed in other perovskite oxide p-n junctions, such as (Pb, La)$(Zr,Ti)O_3$/Nb–$SrTiO_3$.[19] It is worth to note: unlike the hysteresis due to the dielectric relaxation or trapped carriers at low field as shown in the inset of Fig. 3, the current flows more during decreasing $|V|$ rather than increasing $|V|$, which is very much similar as that found in the contaminated Schottky barriers on Si.[20] Another interesting feature in Fig. 3 is the strong dopant dependence of I-V characteristics. Current density of Mn-doped film is dramatically reduced by two orders of magnitude, while current density of BNBT-LaCe film just reduces slightly compared with that of undoped film. It has been reported that the Mn doping is effective to lower the leakage current in $BiFeO_3$ and $(K,Na)NbO_3$ by suppressing of intrinsic p-type conductivity of undoped films.[21,22] This is associated with decreasing the total number of free carriers (holes) that correlated with the A-site vacan-

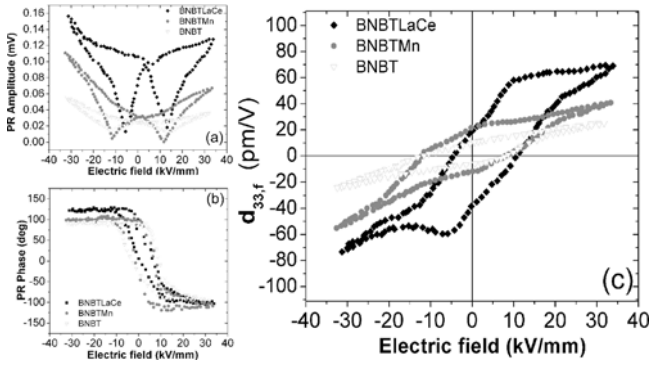

FIG. 4. (Color online) Local piezoresponse (a) amplitude, (b) phase, and (c) effective $d_{33,f}$ hysteresis loops of the epitaxial BNBT-based thin films measured at room temperature.

cies. In our Mn-doped BNBT thin films, similar phenomena could be achieved, as Mn^{2+} ($r \sim 0.90$ Å) possesses close ionic radius to Na^{+} ($r \sim 1.02$ Å) and Bi^{3+} ($r \sim 1.03$ Å), thus very likely occupies the *A*-site vacancies. In the La+Ce codoped film, however, Ce^{3+} ($r \sim 1.02$ Å) and La^{3+} ($r \sim 1.03$ Å) may not only compensate the existing *A*-site vacancies but also possibly substitute Ba^{2+} ($r \sim 1.35$ Å) to create extra *A*-site vacancies, resulting in the leakage current is insignificantly reduced as compared with the undoped film.

The local d_{33} piezoelectric hysteresis loops were measured by piezoforce microscopy (PFM) (Digital Instruments, NanoScope IV, Plainview, NY) incorporated with a lock-in technique.[23] Details of the local d_{33} loop measurements were described in our previous work.[10] Figures 4(a) and 4(b) display the variations of the static piezoresponse (PR) amplitude (A) and phase (Φ), respectively, with the bias dc electric field for a grain of the thin films at room temperature. The effective $d_{33,f}$ were derived from $d_{33,f}=A\cdot\cos\Phi$, as shown in Fig. 4(c). The amplitude of static PR [Fig. 4(a)] exhibits a typical well-shaped "butterfly" loop, while the d_{33} hysteresis loops are distorted and offset. The offset of d_{33} hysteresis loops could be attributed to the presence of nonswitchable domains pinned near the electrode-film interface and built-in electric field (imprint),[24,25] which results from the difference nature of the top and bottom electrodes: the Pt/Ir tip serves as the top electrode whereas the bottom electrode consists of epitaxial CRO. Values of maximum and remanent $d_{33,f}$ were found to be 70 and 31 pm/V, 48 and 18.5 pm/V, and 26 and 10.5 pm/V for BNBTLaCe, BNBTMn, and pure BNBT thin films, respectively. It can be seen that the dopants have remarkably enhanced the piezoelectric properties of BNBT thin films. In consistence with its good ferroelectricity, the promising piezoelectric performance in BNBTLaCe thin film is attributed to the ease of domain wall movement induced by the *A*-site substitutions. Although Mn may also act as an *A*-site dopant, its "hardening effect" by compensating *A*-site vacancies and substituting *B*-site ions partially smears its contribution on facilitation of movement of domain walls, resulting in a relatively lower apparent piezoelectric coefficient. Owing to the clamping effect imposed by the substrates, the piezoelectric coefficients in doped BNBT thin films are much lower than their bulk values (~160 pC/N). However, the observed $d_{33,f}$ value for BNETLace film is very much comparable to those of the lead-based counterparts ($d_{33,f}=10-110$ pm/V for typical PZT thin films[26]) and one of the highest reported values for lead-free piezoelectric thin films up to this date. In addition, we believe the ferroelectric and piezoelectric properties of these BNBT-based thin films can be further enhanced through judicious control of doping level, as the MPB and optimal doping concentration in thin film forms might be slightly different from those of bulks.

In summary, this study investigated the doping effects on electrical properties of BNBT-based thin films with the composition in the vicinity of MPB grown on $CaRuO_3$ coated LSAT (001) substrates by pulsed laser deposition. It has been shown that La+Ce codopants are more effective to enhance the ferroelectric, dielectric, and piezoelectric properties by introducing extra *A*-site vacancies to facilitate the domain wall movement, whereas Mn doping is more favorite to reduce the leakage current by two order of magnitude as compared to the undoped thin film. All the films exhibited diode-like *I-V* characteristics, owing to their oxide *p-n* junction type heterostructures. Our results suggest that the doped BNBT-based lead-free thin films may have great potential for future applications in environmentally friendly nonvolatile memories and piezoelectric devices.

This work was supported by the Vice-Chancellor's postdoctoral fellowship program of the University of New South Wales (Grant Nos. SIR50/PS16940 and SIR30/PS20198).

[1] P. K. Panda, J. Mater. Sci. **44**, 5049 (2009).
[2] G. A. Smolenskii, V. A. Isupov, A. I. Agranovskaya, and N. N. Krainik, Sov. Phys. Solid State **2**, 2651 (1961).
[3] J. Suchanicz and W. S. Ptak, Ferroelectr., Lett. Sect. **12**, 71 (1990).
[4] T. Takenaka, K. Maruyama, and K. Sakata, Jpn. J. Appl. Phys., Part 1 **30**, 2236 (1991).
[5] Y. Hiruma, H. Nagata, and T. Takenaka, Jpn. J. Appl. Phys., Part 1 **45**, 7409 (2006).
[6] X. X. Wang, H. L. W. Chan, and C. L. Choy, Appl. Phys. A: Mater. Sci. Process. **80**, 333 (2005).
[7] X. Y. Zhou, H. S. Gu, Y. Wang, W. Y. Li, and T. S. Zhou, Mater. Lett. **59**, 1649 (2005).
[8] X. G. Tang, J. Wang, X. X. Wang, and H. L. W. Chan, Chem. Mater. **16**, 5293 (2004).
[9] H. W. Cheng, X. J. Zhang, S. T. Zhang, Y. Feng, Y. F. Chen, Z. G. Liu, and G. X. Cheng, Appl. Phys. Lett. **85**, 2319 (2004).
[10] D. Y. Wang, D. M. Lin, K. S. Wong, K. W. Kwok, J. Y. Dai, and H. L. W. Chan, Appl. Phys. Lett. **92**, 222909 (2008).
[11] D. Alonso-Sanjosé, R. Jimenez, I. Bretos, and M. L. Calzada, J. Am. Ceram. Soc. **92**, 2218 (2009).
[12] M. Bousquet, J. R. Duclere, C. Champeaux, A. Boulle, P. Marchet, A. Catherinot, A. Wu, P. M. Vilarinho, S. Deputier, M. Guilloux-Viry, A. Crunteanu, B. Gautier, D. Albertini, and C. Bachelet, J. Appl. Phys. **107**, 034102 (2010).
[13] M. Abazari, A. Safari, S. S. N. Bharadwaja, and S. Trolier-McKinstry, Appl. Phys. Lett. **96**, 082903 (2010).
[14] R. J. Kennedy, R. Madden, and P. A. Stampe, J. Phys. D: Appl. Phys. **34**, 1853 (2001).
[15] A. Ito, H. Masumoto, and T. Goto, J. Ceram. Soc. Jpn. **115**, 683 (2007).
[16] D. Damjanovic, Rep. Prog. Phys. **61**, 1267 (1998).
[17] S. Valencia, A. Gaupp, and W. Gudat, Phys. Rev. B **73**, 104402 (2006).
[18] M. Abazari and A. Safari, J. Appl. Phys. **105**, 094101 (2009).
[19] Y. Watanabe, Phys. Rev. B **59**, 11257 (1999).
[20] Y. Watanabe, Ferroelectrics **349**, 190 (2007).
[21] S. K. Singh, H. Ishiwara, and K. Maruyama, Appl. Phys. Lett. **88**, 262908 (2006).
[22] M. Abazari, E. K. Akdoğan, and A. Safari, Appl. Phys. Lett. **92**, 212903 (2008).
[23] G. Zavala, J. H. Fendler, and S. Trolier-McKinstry, J. Appl. Phys. **81**, 7480 (1997).
[24] A. L. Kholkin, E. L. Colla, A. K. Tagantsev, D. V. Taylor, and N. Setter, Appl. Phys. Lett. **68**, 2577 (1996).
[25] S. V. Kalinin, B. J. Rodriguez, S. Jesse, E. Karapetian, B. Mirman, E. A. Eliseev, and A. N. Morozovska, Annu. Rev. Mater. Res. **37**, 189 (2007).
[26] P. Muralt, IEEE Trans. Ultrason. Ferroelectr. Freq. Control **47**, 903 (2000).